Environmental Technology & Innovation 38 (2025) 104133

Contents lists available at ScienceDirect

Environmental Technology & Innovation

journal homepage: www.elsevier.com/locate/eti

Engineered biochar effects on methane emissions and rice yield under alternate wetting and drying in paddy soils

Chang Liu [a,d], Taotao Chen [a,b,c], Feng Zhang [a], Hongwei Han [a], Benji Yi [a], Jun Meng [b,c], Daocai Chi [a,*], Yong Sik Ok [d,**]

[a] College of Water Conservancy, Shenyang Agricultural University, Shenyang 110866, China
[b] National Biochar Institute, Shenyang Agricultural University, Shenyang 110866, China
[c] Key Laboratory of Biochar and Soil Improvement, Ministry of Agriculture and Rural Affairs, Shenyang 110866, China
[d] Korea Biochar Research Centre, Division of Environmental Science and Ecological Engineering, Korea University, Seoul 02841, Republic of Korea

ARTICLE INFO

Keywords:
Acid modified biochar
CH_4 emissions
AWD
Soil degradation
Climate change mitigation
Rice production

ABSTRACT

Biochar is a promising strategy for improving crop yield and mitigating greenhouse gas emissions. However, the impacts of acid modified biochar on CH_4 emissions and yield in rice fields are not comprehensively understood, especially under alternate wetting and drying irrigation (I_{AWD}). Here, we conducted a 3-yr (2019-2021) field experiment with two irrigation regimes (I_{CF}: continuous flooding irrigation, I_{AWD}) and three biochar treatments (B_0: no biochar; B_{20}: 20 t ha^{-1} rice straw biochar; and B_{20A}: 20 t ha^{-1} acid modified rice straw biochar). Results showed I_{AWD} reduced CH_4 emissions by 63–80 % and water consumption by 10–12 % but threatened the rice soil fertility. B_{20} and B_{20A} increased soil cation exchange capacity by 13–36 %, soil organic carbon by 24–44 % and C/N by 17–36 % over the three years. However, compared to B_0, B_{20} tended to increase CH_4 emissions and factor (CH_{4EF}), reduced grain yield by 6 % in 2019, but B_{20A} suppressed CH_4 emissions by 19 % while maintaining a stable grain yield. B_{20} and B_{20A} enhanced yield by 5 % and 8 %, 11 % and 12 % and decreased CH_4 emissions by 22 % and 38 %, 38 % and 40 % in 2020 and 2021, respectively. B_{20A} alleviated its initial negative impact on CH_4 emissions and yield in 2019 due to acid modified biochar enhancing more acidic and oxygenated functional groups. $I_{AWD}B_{20A}$ decreased CH_4 emissions by 75–89 % and greenhouse gas emission intensity (GHGI) by 75–90 % compared to $I_{CF}B_0$ over the three years. Consequently, B_{20A} coupled with I_{AWD} achieves sustainable use of water resources, improves soil degradation and mitigates climate change.

1. Introduction

Rice is a major cereal crop, feeding over 50 % of the world's population. However, rice fields account for about 48 % of greenhouse gas (GHG) emissions from croplands. CH_4 emissions from paddy field contribute to more 75 % of its total GHG emissions due to the anaerobic environment with long-term waterlogged conditions. China, as one of the major rice-producing countries, has prominent positions in total anthropogenic CH_4 emissions, accounting for 22–38 % of the global emissions (Nikolaisen et al., 2023; Qian et al.,

* Correspondence to: Shenyang Agricultural University, Shenyang 110866, China.
** Corresponding author.
E-mail addresses: chidaocai@syau.edu.cn (D. Chi), yongsikok@korea.ac.kr (Y.S. Ok).

https://doi.org/10.1016/j.eti.2025.104133
Received 23 September 2024; Received in revised form 20 January 2025; Accepted 4 March 2025
Available online 5 March 2025

2023; Wang et al., 2019). This is a huge challenge for China's goal of "a carbon peak by 2030 and carbon neutrality by 2060" (Liu et al., 2024). On the other hand, rice in China contributes to 21.4 % of the global production to meet food needs, but its production also consumes large amounts of water, accounting for 70 % of China's agricultural water consumption. This is undoubtedly another serious challenge for China, which is facing increasing water shortages (Liu et al., 2021; Han et al., 2023a; Li et al., 2024). With the dual challenges of climate change and water scarcity, exploring potential measures for reducing water use and CH_4 emission in rice fields, while maintaining rice yields, is essential to achieve GHG emissions reduction and sustainable development of China's agriculture.

Alternate wetting and drying irrigation (I_{AWD}) is a vital strategy for improving water use efficiency (WUE) and mitigating CH_4 emissions in rice fields, which has been widely applied in China (Chen et al., 2022; Chu et al., 2018). Studies indicated that I_{AWD} decreased water consumption by 12 %-14 % and increased WUE by 10 %-24 % compared to continuous flooding (Han et al., 2023a; Li et al., 2022; Carrijo et al., 2017). As rice soils become unsaturated, aerobic conditions prevail under I_{AWD}, resulting in a high O_2 soil environment that promoted CH_4 oxidation and inhibited CH_4 emissions (Han et al., 2023b). However, Livsey et al. (2019) reported that I_{AWD} improved soil aeration, which led to a loss of soil organic carbon (SOC), with a 5.2 % reduction in SOC concentration compared to I_{CF}. SOC plays a vital role in enhancing soil fertility, which in turn affects rice yield. Consequently, the loss of SOC may result in rice reduction (Berhane et al., 2020). Chen et al. (2022) also discovered that I_{AWD} increased N_2O emissions due to high redox potential and nitrate nitrogen concentration, leading to an 8–15 % increase in gaseous nitrogen losses. In short, while I_{AWD} reduces water consumption and CH_4 emissions, the resulting decline in soil fertility, reduction in crop yield and loss of nitrogen cannot be ignored.

Both zeolite amendment and biochar incorporation into agricultural soil were widely used as potential strategies to achieve crop yields enhancement and GHG emissions reduction while improving soil fertility (Livsey et al., 2019; Zhao et al., 2024). Rice straw, as the second most abundant straw resources in China, accounting for 25 % of the straw output of main crops, and a large number of rice straw are directly burned, resulting in resource waste and environmental pollution (Ai et al., 2015; Sharma et al., 2020). The shift from rice straw into biochar is one of the most widely used measures for efficient utilization of straw resources, which directly and indirectly avoid carbon emissions from straw burning or straw rotting and sequestrate those carbon in soil directly instead. With its high specific surface area and cation exchange capacity (CEC), biochar improves soil fertility, soil sequestration and reduces emissions, achieving the green and low-carbon goal of "taking from the field and using it to the field". Consequently, biochar has become a major research focus for many scientists in recent years (Nan et al., 2022; Han et al., 2023a). Sriphirom et al. (2020) found that biochar increased soil SOC by 21.2 % over two rice growing seasons, indicating that biochar has a strong carbon sequestration capacity. He et al. (2020) demonstrated that long-term successive biochar incorporation in rice-wheat rotation had a considerable potential to reduce N_2O emissions, especially during the rice season. However, Yang et al. (2020) observed that biochar increased CH_4 emissions in the 1st year but reduced in the 2nd year, probably due to biochar progressive degradation and aging, which considerably altered the abundance of methanogens and methanogenic bacteria through increased pH value. Major et al. (2010) found that biochar (20 t ha^{-1}) had no effect on maize yield in the first year but increased in subsequent years because of that biochar had more significant effects on soil nutrients (P and K) as time goes. Furthermore, Zhang et al. (2023) demonstrated that the properties of biochar itself created a loose and porous environment for the rice roots, which was conducive to retaining water and nutrient retention, facilitating root growth and enhancing methane oxidation, thereby reducing CH_4 emissions. In summary, an increasing number of studies have found that initial biochar incorporation, the lime effect and the nutrient effect caused by an increase in pH have no positive influence on CH_4 and grain yield, or even a negative influence, reducing production and increasing emissions. Whereas, with aging of biochar, its influence on soil properties and microbial activity changes, resulting in different impacts (Duan et al., 2018; Nan et al., 2022; Wu et al., 2022). Therefore, it is necessary to solve the negative effects of the initial pH increase of biochar to fully realize its potential as a carbon sink, emission reduction and stable production to achieve green sustainable development, especially under I_{AWD}.

The production process of acid modified biochar is simple and typically involves the acidification of fresh biochar with HCl, HNO_3, H_2SO_4 and H_3PO_4 (Rehman et al., 2020). This has become one of the most effective measures to address the initial negative effects of biochar. Engineered biochar with acid modification exhibited obvious loose structure and abundant pore structure, included more oxygen-containing functional groups and acidic functional groups (Yu et al., 2023). These changes directly alter the properties of the soil environment and microbial activity, playing a key role in increasing crop growth and mitigating greenhouse gas emissions (Gong et al., 2024; Chen et al., 2022). On the one hand, acid modified biochar exhibited larger specific surface area and higher water-holding capacity, which reduced nutrient loss and improved aboveground dry matter and crop yields (Li et al., 2025; Yu et al., 2023; Sahin et al., 2017). On the other hand, acid modified biochar significantly reduced pH value, promoted microbial electron transfer, increased the content of oxygen-containing functional groups with redox activity, and performed better redox capacity, thus inhibiting the activity of methanogens and reducing CH_4 emissions of rice soil in the laboratory (Nan et al., 2021). However, both acid type and concentration were two of the critical determinant factors affecting the mechanism of functional groups' oxidation of biochar during the related acidification processes. H_3PO_4, as a lower corrosivity among those acidic agents, can introduce some P-containing functional groups (e. g., C_3-P-O, P-OOH, and P-O-P) to biochar but decrease oxygen-containing functional groups (Sajjadi et al., 2019). The number of carboxyl and acidic functional groups (C═O) on the rice straw biochar modified by HNO_3/H_2SO_4 increased significantly compared with that treated by HCl acidification (He et al., 2022; Chen et al., 2024; Kasera et al., 2022). However, after the dissociation of HNO_3, a very active intermediate nitrate (NO_2^+) will form -NO_2 on the surface of biochar, resulting in limited nitrification on its surface. But H_2SO_4 can enhance the formation of nitrate ions and improve its adsorption capacity (Godwin et al., 2019). Studies have proved that HCl, HNO_3 and H_2SO_4 treated biochar, among which H_2SO_4 treated biochar has the best acidification effect, and with the increase of acid concentration (0.1–1 M), the number of acidic functional groups (lactic acid functional groups) increases from 9 % to 15 % (Boguta et al., 2019). However, the concentration of H_2SO_4 is too high, which caused a detrimental impact on the micropore surface area of biochar (Sajjadi et al., 2019). Therefore, the best acid modified effect of biochar can be optimized by the appropriate acid concentration. At present, acid modified biochar has mostly been used to remove pollutants in water and heavy metals in soil, and the experiments have mostly been carried out in laboratories or potted plants (Ashworth et al., 2023; Gong et al., 2024). However, studying its impacts on rice field remains largely unexplored, especially under I_{AWD}. A deeper exploration of acid modified biochar incorporation in AWD paddy fields and the impacts of fresh and acidified biochar on soil properties, rice yield and CH_4 emissions are essential to reveal whether acid modified biochar's can alleviate the negative effects of the initial lime effect of biochar and realize low carbon production.

Therefore, we applied both straw biochar and acid modified biochar to AWD paddy fields to assess its impacts on CH_4 emissions, soil properties, water use efficiency and grain yield. This study was conducted with the following objectives: (i) evaluate alternations in the structure and morphological characteristics of biochar after its acid modification; (ii) monitor and assess the contrasting differences in soil environment, CH_4 emission, grain yield in paddy field under different biochar treatment under AWD; (iii) reveal potential possibility regarding the acid modification of biochar whether to alleviate biochar-induced initial CH_4 emissions and yield decrease, realizing low carbon production under alternate wetting and drying rice paddy. This research is important in effectively mitigating GHG emissions and achieving low carbon and promoting rice sustainable development.

2. Materials and methods

2.1. Experimental site and materials

The field experiment was conducted at the National Demonstration Base of Shenyang Agricultural University, located in Shenyang, Liaoning Province (latitude N 41°52', longitude E 122°67') from 2019 to 2021. Daily precipitation and air temperature during the three rice growing seasons were shown in Fig. S1. Local Japonica rice cultivar (Dalinuo 1) was used in 2019 and 2020, but due to the force majeure of the epidemic, the rice cultivar was changed to Shennong 09001 in 2021. Detailed information on rice cultivation was described in Table S1. The experimental site features silt loam topsoil from river alluvium. Fresh biochar was produced by pyrolyzing rice straw at 500 °C for 2 hours. To produce acid modified biochar, fresh biochar was hydrolyzed by soaking in 0.5 N H_2SO_4 (1:20 ratio) for 24 h and acidified, then washed repeatedly with water until its pH was in the range of 6.5–7.5 and finally dried at 60 °C for 48 h. The physical and chemical properties of the pre-experiment topsoil, biochar and acid modified biochar were given in Table S2.

2.2. Experimental design and management practices

A split-plot design with two irrigation regimes, three biochar treatments and three replications were used in this field experiment. Irrigation regimes (I) as main plots, including continuous flooding (I_{CF}) and alternative wetting and drying (I_{AWD}). Sub plots were subjected to three biochar treatments (B) (no biochar, B_0, 20 t ha^{-1} fresh biochar, B_{20} and 20 t ha^{-1} acid modified biochar, B_{20A}). This results in a total of six treatments ($I_{CF}B_0$, $I_{CF}B_{20}$, $I_{CF}B_{20A}$, $I_{AWD}B_0$, $I_{AWD}B_{20}$ and $I_{AWD}B_{20A}$) (Fig. S2). The main plots were subdivided by 100 cm wide soil ridges, with each subplot separated by a 40 cm deep polyvinyl chloride barrier embedded 30 cm into the soil to limit horizontal nutrient flow. Each plot was 3 m in width and 6 m in length. Water supply lines and meters were installed in each plot to manage soil moisture.

Under both I_{CF} and I_{AWD}, a standing water depth of 10–30 mm was maintained for the first 7–10 days after transplanting to aid seedling recovery. Subsequently, I_{CF} plots were kept at a water depth of 10–70 mm until about 15 days before harvest. Under I_{AWD}, the plots were re-flooded to 70 mm, reducing soil water potential to −10 kPa at a 15 cm soil depth. These I_{AWD} cycles persisted until roughly 15 days before harvest.

An automatic ultrasonic water level meter (AODC-SY001-APD2, Fujian, China) recorded water levels hourly. Soil water potential at a depth of 15 cm in each I_{AWD} plot was measured twice daily (8:00 am and 2:00 pm) using a soil moisture tension meter (HX-S-10, Institute of Soil Science, Nanjing, China). Fertilizer application was consistent with local agricultural practices, with specifics detailed in Table S1. The experiment was replicated in the following two years without biochar. Weed, pesticide, and pest management practices followed local rice cultivation guidelines.

2.3. CH_4 sampling collection

CH_4 fluxes were measured using the opaque static chamber method (Zhao et al., 2024). Each chamber constructed from PVC with a 0.7 (l) × 0.5 (w) × 0.6 (h) m standard chamber and 0.7 (l) × 0.5 (w) × 1.1 (h) m extension chamber. To ensure gases mixing and stable temperature, a digital thermometer and a fan were installed on top of the chamber. CH_4 gas samples were typically collected roughly once a week (9:00–11:00 am). An additional sample was taken after each fertilizer application, dry and wet cycle and rainfall event. Gases were extracted from the chamber into a 150 mL vacuum aluminum bag by using a 100 mL syringe at 0, 15, and 30 min. CH_4 concentrations were determined with a gas chromatograph (Agilent 7890B, Agilent Technologies, USA) equipped with Flame Ionization Detector (FID).

2.4. Soil and plants analysis

After transplanting, three topsoil samples were taken once a week from each plot using an auger and thoroughly mixed to form a fresh soil sample to measure soil NH_4^+-N and NO_3^--N concentrations using the AA3 (Seal Analytical, Auto-analyzer 3, Germany). Air-dried soil samples were analyzed for soil organic carbon (SOC) and soil cation exchange capacity (CEC). Potassium dichromate-sulphuric acid digestion method was used to measure SOC (Shen and Yu., 2021). CEC was determined using a DIGIPREP TKN

System (K-360, BUCHI Labortechnik AG 9230 Flawil, Switzerland). Soil redox potential (Eh), temperature and pH were measured in situ with an automatic redox potential tester (CN61M/FJA3, Nanjing, China) at the same sampling intervals as CH_4 samplings. Soil particle size distribution was analyzed with a laser particle size analyzer (MAETERSIZER 3000, Britain) (Wang et al., 2023).

After harvesting, each soil sample (0.2 m × 0.2 m × 0.2 m) containing rice roots was carefully excavated, a 100-mesh nylon belt was placed under the root of the plant and the roots were carefully separated from the soil by washing with tap water. Images were analyzed using WINRHIZO software (WinRHIZO Pro LA2400, Regent Instruments Inc., Quebec, Canada). Root diameter and root length density were determined using a flatbed scanner (EU-88, SEIKO EPSON CROP, Japan) (Chen et al., 2019). Oven drying was used to determine root and above-ground dry weights.

2.5. Biochar characterization

Fourier Transform Infrared Spectrometer (FTIR) (Spectrum 3, Perkin Elmer, USA) was used to understand the surface functional groups of B_{20} and B_{20A} (Han et al., 2023a). CEC was measured using a DIGIPREP TKN System (K-360, BUCHI Labortechnik AG 9230 Flawil, Switzerland). C/N was determined by elemental analyzer (PerkinElmer 2400, Waltham, MA, USA). The morphological feature of the biochar was characterized by a scanning electron microscope (FE-SEM, APREO 2 C, THERMELFELD, USA). Raman spectra were captured by using a Raman Microscope (DXR, THERMO, USA).

2.6. Calculation of the data

CH_4 fluxes were calculated as follows:

$$F = \rho \cdot h \cdot \frac{dC}{dt} \cdot \frac{273}{273 + T} \cdot \frac{p}{p_0} \tag{1}$$

where F is the CH_4 flux (mg m^{-2} h^{-1}); ρ is the gas density of CH_4 (0.714 kg m^{-3}); h is the chamber height; T is the average air temperature in the chamber (°C); dC/dt is the linear change in CH_4 gases concentration over time (mg L^{-1} h^{-1}). p is air pressure inside the chamber, and p_0 is the standard atmospheric pressure.

Cumulative CH_4 emissions were calculated as follows:

$$f = \sum_{i=1}^{n} \frac{F_i + F_{i-1}}{2} \cdot d \cdot 24 \cdot 10^{-2} \tag{2}$$

where f is the cumulative CH_4 (kg ha^{-1}) emission; F_i and F_{i-1} are the gas fluxes of two consecutive samples; d is the interval in days between two consecutive samples, and n is the sum of gases samples.

The CH_4 emission factor is the average daily CH_4 emission rate during the rice growth season. It was calculated as follows (Sun et al., 2020):

$$EFc = \frac{f}{D} \tag{3}$$

where EFc is the CH_4 emission factor (kg CH_4 ha^{-1} d^{-1}), f is the total seasonal CH_4 emission (kg CH_4 ha^{-1}), and D is the rice growth season (day).

Global warming potential of CH_4 (GWP_{CH_4}) was calculated using the following equation (Forster et al., 2021):

$$GWP_{CH_4} = 27.2 \times CH_4 \tag{4}$$

where CH_4 represents the cumulative CH_4 emissions (kg ha^{-1}). The value 27.2 indicates that the GWP_{CH_4} has a global warming potential 27.2 times greater than carbon dioxide (CO_2) per unit mass over a 100-year period.

The Greenhouse Gas Intensity ($GHGI_{CH_4}$) was calculated as follows:

$$GHGI_{CH_4} = \frac{GWP_{CH_4}}{Y} \tag{5}$$

where GWP_{CH_4} is global warming potential of CH_4 emissions, Y represents yield (t ha^{-1}).

Water use efficiency (WUE) was calculated as follows:

$$WUE = \frac{Y}{I_t} \tag{6}$$

where Y is the rice yield (t ha^{-1}), I_t is the total amount of irrigation water during the rice growth season.

Root length density (RLD) was calculated using the following equation (Ding et al., 2021):

$$RLD = \frac{L}{V_s} \tag{7}$$

where L is the root length (cm), V_s is the volume of soil samples with rice roots (cm^{-3}).

2.7. Statistical analysis

Analysis of variance for all data were analyzed using R software (release 4.3.1) in a split-plot design. The irrigation regime and the incorporation of biochar were considered as fixed effects and the replications as random effects. Before performing ANOVA, data that did not fit normally were log transformed. Multiple comparisons were performed using the Tukey's HSD test at the $P < 0.05$ level. All significant differences are at the $P < 0.05$ level, unless otherwise stated (Liu et al., 2019). Path analysis was conducted to assess the contribution of related factors to CH_4 emissions using IBM SPSS (Version 21, USA). All figures were plotted with OriginPro 2024.

3. Results

3.1. Biochar characterization

Cation exchange capacity (CEC), pH value and C/N under B_{20} and B_{20A} were shown in Fig. S3. B_{20A} reduced CEC by 15.4 % compared to B_{20} (30.52 cmol kg^{-1} vs 36.07 cmol kg^{-1}), but both had a higher CEC compared to the biochar-free control (soil) (16.85 cmol kg^{-1}) before transplanting. B_{20A} had a relative higher C/N, which increased C/N by 7.2 % over B_{20} (48.32). After washing with 0.5 N H_2SO_4, B_{20A} reduced pH value from 10.14 to 7.01 (Fig. S3; Table. S2).

The SEM images of B_{20} and B_{20A} were revealed in Fig. S4a-b. B_{20} showed a sieve-like structure, with a rough and less particulate matter. Compared with B_{20} (Fig. S4a), B_{20A} exhibited abundant pore structures and some irregularly shaped particles on the surface. Pore wall destruction and smoother surface of biochar can be seen after acid modification (Fig. S4b).

FTIR spectroscopy indicated that B_{20} and B_{20A} consistently showed three obvious characteristic peaks, including phenolic hydroxyl group represented by -OH (2500–4000 cm^{-1}), carboxyl group expressed as C=O and C=C (1200–1900 cm^{-1}), and aromatics and alkanes represented by C-O (1050–1150 cm^{-1}) (Fig. S4c). However, B_{20A} was higher in -OH (3440 cm^{-1}) and C=O (1630 cm^{-1}) absorption peaks and oxygenated functional groups relative to B_{20}. The increase in these functional groups resulted in higher adsorption and ion exchange capacity and lower soil pH.

Raman (Fig. S4d) spectroscopy was conducted on the B_{20} and B_{20A} to study the characterization of the defects. Two distinct peaks at 1350 cm^{-1} and 1590 cm^{-1} are corresponding to the D and the G bands, respectively. Usually, I_D represented the D band for sp^2 disordered carbon, positioned from 1320 to 1365 cm^{-1}. I_G represented the G band for sp^2 graphitic carbon, positioned from 1520 to 1600 cm^{-1}. I_D/I_G can reflect the degree of biochar defects. The I_D/I_G of B_{20} and B_{20A} are 0.75 and 0.82, respectively (Fig. S4d).

Table 1
Means and ANOVAs for soil NH_4^+-N, and NO_3^--N, pH, Eh, temperature, and SOC during the 2019, 2020, and 2021 rice growing season.

Season	Treatments	Soil NH_4^+-N (mg kg^{-1})	Soil NO_3^--N (mg kg^{-1})	Soil pH	Soil Eh (mV)	Soil temperature (℃)	SOC (g kg^{-1})
2019	I_{CF}	28.74 ± 3.14a	0.51 ± 0.04b	6.52 ± 0.10a	136.92 ± 6.22b	23.54 ± 0.41a	13.17 ± 2.48 a
	I_{AWD}	31.21 ± 3.30a	0.61 ± 0.07a	6.53 ± 0.13a	234.41 ± 14.06a	23.56 ± 0.32a	13.85 ± 2.08a
	B_0	28.56 ± 3.19b	0.54 ± 0.07b	6.44 ± 0.04b	182.25 ± 52.10a	23.47 ± 0.30b	10.88 ± 0.73c
	B_{20}	28.27 ± 3.09b	0.54 ± 0.06b	6.67 ± 0.04a	183.88 ± 55.50a	23.81 ± 0.35a	14.02 ± 1.24b
	B_{20A}	33.10 ± 1.14a	0.61 ± 0.09a	6.46 ± 0.03b	190.76 ± 55.58a	23.36 ± 0.29b	15.62 ± 1.09a
	ANOVAs						
	I	ns	*	ns	*	ns	ns
	B	* *	*	* *	ns	*	* *
	I×B	ns	ns	ns	ns	ns	ns
2020	I_{CF}	20.66 ± 2.39a	0.45 ± 0.03b	6.36 ± 0.03b	122.96 ± 12.47b	22.32 ± 0.49a	15.92 ± 2.84a
	I_{AWD}	23.90 ± 1.79a	0.55 ± 0.03a	6.42 ± 0.05a	234.76 ± 9.48a	22.71 ± 0.39a	16.98 ± 2.00a
	B_0	20.57 ± 2.85b	0.50 ± 0.07a	6.40 ± 0.06a	179.73 ± 65.13a	22.36 ± 0.35a	13.54 ± 1.21b
	B_{20}	23.09 ± 2.65a	0.50 ± 0.06a	6.41 ± 0.05a	173.29 ± 61.99a	22.69 ± 0.62a	17.36 ± 1.54a
	B_{20A}	23.18 ± 1.82a	0.51 ± 0.05a	6.37 ± 0.04a	183.56 ± 59.11a	22.50 ± 0.44a	18.46 ± 0.68a
	ANOVAs						
	I	ns	* *	*	* *	ns	ns
	B	*	ns	ns	ns	ns	* *
	I×B	ns	ns	ns	ns	ns	ns
2021	I_{CF}	30.13 ± 1.96a	1.40 ± 0.12b	6.26 ± 0.05b	113.91 ± 8.50b	22.26 ± 0.19a	17.44 ± 1.91a
	I_{AWD}	29.16 ± 4.37a	1.55 ± 0.08a	6.42 ± 0.03a	233.79 ± 10.93a	22.46 ± 0.15a	17.96 ± 2.23a
	B_0	26.14 ± 3.41b	1.37 ± 0.14b	6.33 ± 0.11a	170.69 ± 62.98a	22.33 ± 0.26a	15.14 ± 0.85b
	B_{20}	31.12 ± 1.13a	1.53 ± 0.05a	6.34 ± 0.09a	171.71 ± 66.14a	22.43 ± 0.11a	18.78 ± 0.59a
	B_{20A}	31.68 ± 1.52a	1.53 ± 0.11a	6.36 ± 0.10a	179.15 ± 69.64a	22.32 ± 0.19a	19.18 ± 1.04a
	ANOVAs						
	I	ns	* *	*	* *	ns	ns
	B	* *	* *	ns	ns	ns	* *
	I×B	ns	ns	ns	ns	ns	ns

ANOVAs values were proportion of variance explained by each main effect and interaction. Means ± SD followed by different letters were notably different at $P < 0.05$. I: irrigation regime, B: biochar incorporation. "* *", "* " and "ns" mean significance at $P < 0.01$, $P < 0.05$ and no significance.

3.2. Soil Eh, temperature, pH, SOC and inorganic nitrogen

Seasonal soil Eh was remarkably influenced by irrigation across the three years. I_{AWD} increased soil Eh by 71 %, 91 % and 105 % in 2019, 2020 and 2021, respectively (Table 1). Soil temperature was significantly influenced by biochar in 2019. B_{20} led to an increase in soil temperature (0.34°C) (Table 1). Soil pH was remarkably influenced by biochar in 2019, and by irrigation regime in 2020 and 2021. B_{20} led to an increase in soil pH (0.23 units) in 2019, but not in the following two years, while B_{20A} had a consistent soil pH with B_0 over the three years. Soil pH under I_{AWD} increased by 0.06 units in 2020 and 0.16 units in 2021 (Table 1). Soil organic carbon (SOC) was affected by biochar in the three years. Both B_{20} and B_{20A} increased SOC compared to B_0, while an increase of B_{20A} was higher. B_{20} and B_{20A} increased SOC by 29 % and 44 %, 28 % and 36 %, 24 % and 27 % in 2019, 2020 and 2021, respectively (Table 1).

Seasonal soil NH_4^+-N was remarkably influenced by biochar over three years. Compared to B_0, B_{20} increased it by 12 % in 2020 and 19 % in 2021, while B_{20A} increased soil NH_4^+-N by 16 %, 13 % and 21 % in 2019, 2020 and 2021, respectively. Soil NO_3^--N was significantly influenced by irrigation regime and biochar (except in 2020) in the three years. Soil NO_3^--N under I_{AWD} increased by 20 % in 2019, 21 % in 2020 and 11 % in 2021. B_{20A} increased it by 13 % in 2019 and 12 % in 2021 (Table 1).

3.3. Post-harvest soil CEC and C/N

Both post-harvest soil CEC and C/N were remarkably affected by biochar over three years. B_{20} and B_{20A} had higher soil CEC over B_0, while B_{20A} increased it more, with 20 % in 2019, 13 % in 2020 and 36 % in 2021 (Fig. 1a-c). Compared to B_0, B_{20} significant increased soil C/N by 17 % in 2020 and by 20 % in 2021. However, B_{20A} increased it for three consecutive years, with 36 %, 28 % and 27 %, respectively (Fig. 1d-f).

3.4. Above-ground DMA and root morphological traits

Above-ground DMA was significantly influenced by biochar over the three years and by the I×B interaction in 2020 and 2021. B_{20A} increased DMA by 16 % in 2019, 23 % in 2020 and 15 % in 2021 (Table S4). Among all the treatments, $I_{AWD}B_{20A}$ was 14 %, 28 % and 12 % higher than $I_{CF}B_0$ in 2019, 2020, and 2021, respectively (Fig. 2a). Root dry weight (RDW), diameter (RD) and length density (RLD) were all only significantly influenced by biochar in the three years (Fig. 2b-d). B_{20} had an insignificant increase trend on RDW compared to B_0, but increased it by 28 % in 2020 and 20 % in 2021. While B_{20A} increased RDW by 30 % in 2019, 49 % in 2020 and 37 % in 2021. B_{20} and B_{20A} increased RD by 6 % and 18 % in 2019, 15 % and 21 % in 2020 and 14 % and 18 % in 2021, with B_{20A} significantly increasing RD by 11 % relative to B_{20} in 2019. B_{20} had an insignificant decrease trend on RLD compared to B_0, but B_{20A} increased it by 29 % in 2019. B_{20} and B_{20A} increased RLD by 25 % and 35 % in 2020 and 27 % and 32 % in 2021 (Fig. 2b-d; Table S6).

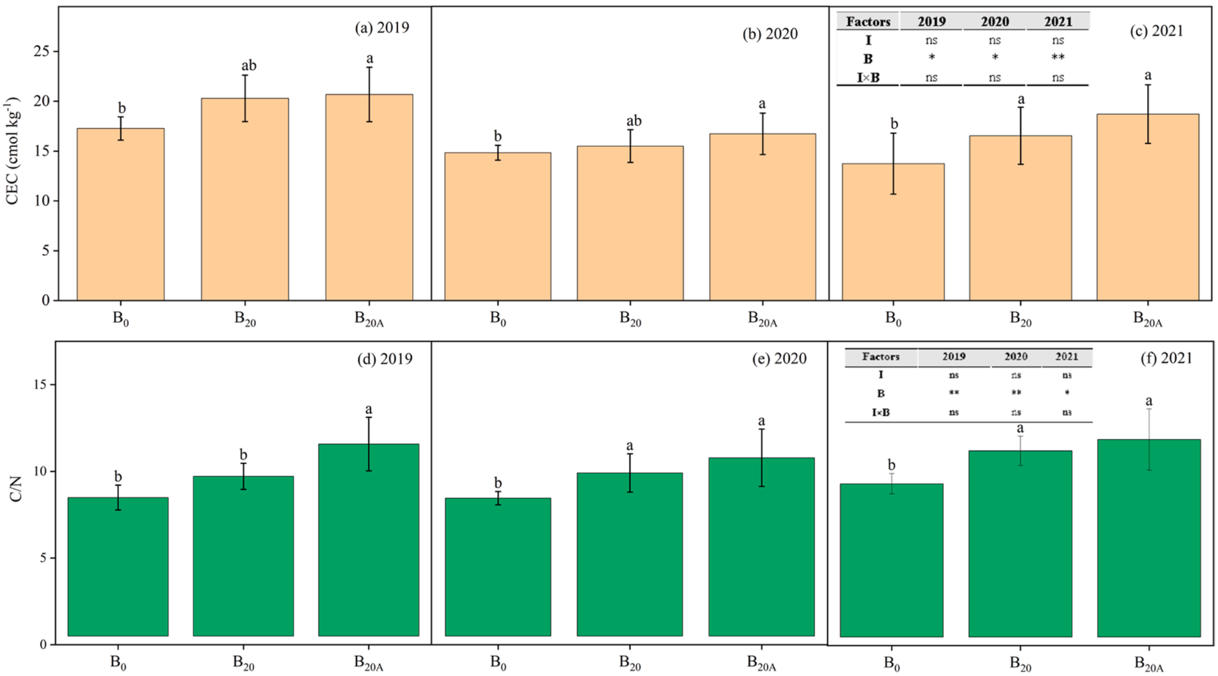

Fig. 1. Influence of irrigation regimes and biochar on post-harvest soil cation exchange capacity (CEC) and C/N in 2019 (a, d), 2020 (b, e) and 2021 (c, f).

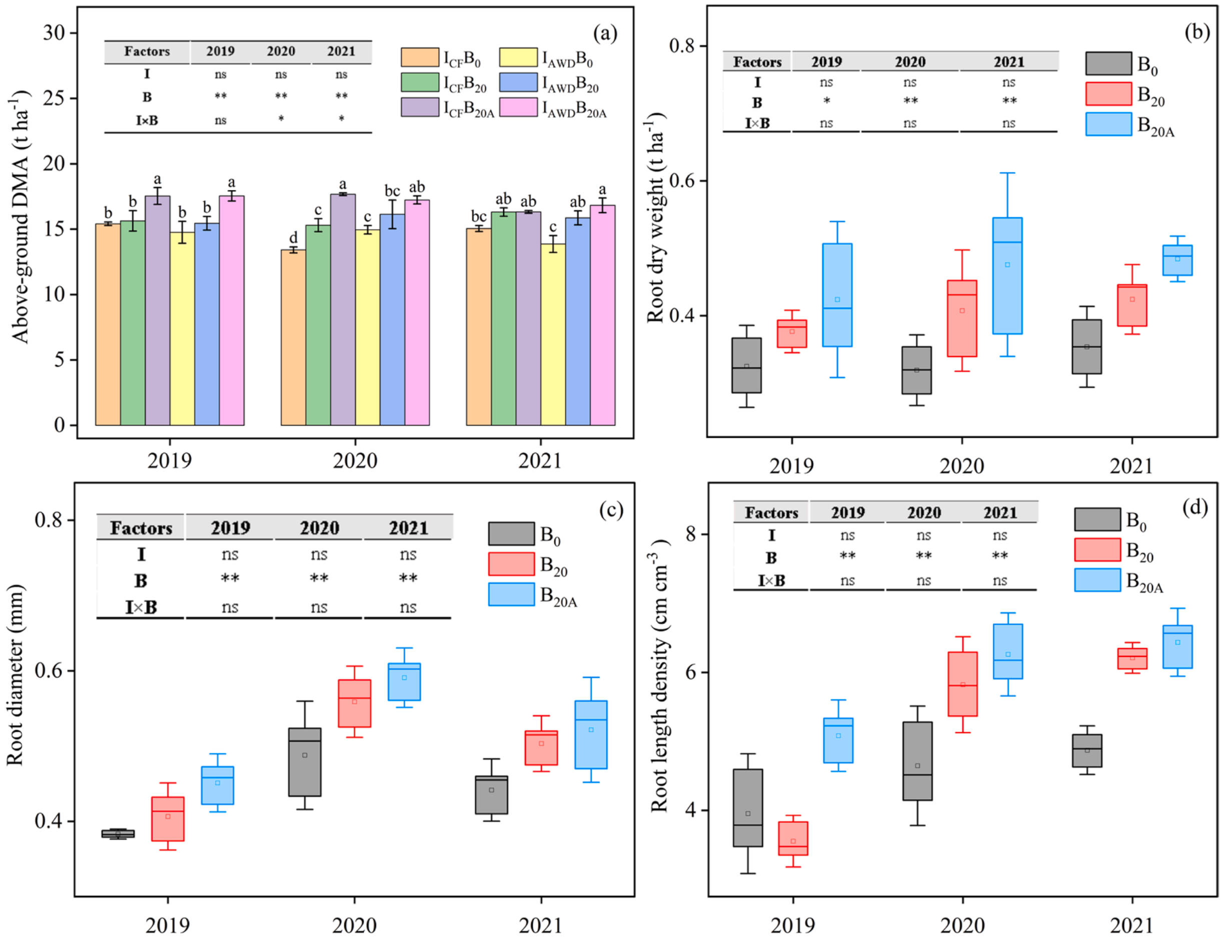

Fig. 2. Impact of irrigation regime and biochar on above-ground DMA (a), root dry weight (RDW) (b), diameter (RD) (c) and length density (RLD) (d) at harvest under six different treatments from 2019 to 2021. I: irrigation regime, B: biochar. * *: $P < 0.01$; * : $P < 0.05$; ns: no significant.

3.5. CH_4 emissions

CH_4 fluxes, ranging from 0.03 to 35.17 in 2019, from −0.05–34.69 in 2020, and from −0.16–25.47 mg m^{-2} h^{-1} in 2021, respectively. It consistently displayed a typical temporal pattern with two notable peaks across all six treatments, with the highest peak occurring 2–7 days after panicle fertilization across the three years. Regardless of biochar application, CH_4 fluxes under I_{AWD} (-0.05–11.40 mg m^{-2} h^{-1}) were significantly lower than those under I_{CF} (-0.16–35.17 mg m^{-2} h^{-1}) in the three years (Fig. 3). CH_4 emissions occurred primarily from 14 days after tillage to 20 days after panicle fertilization, representing 53–64 % of total emissions. I_{AWD} decreased emissions by 46–98 % during this period.

Cumulative CH_4 emissions and CH_4 emissions factors (CH_{4EF}) were remarkably affected by irrigation regime, biochar incorporation, and their interaction (except in 2019) across the three years (Fig. 4a; Table 2). I_{AWD} decreased both CH_4 emissions and CH_{4EF} by 65 % in 2019, 77 % in 2020 and 80 % in 2021. B_{20} was comparable to B_0 and tended to increase, but B_{20A} reduced both cumulative CH_4 emissions and CH_{4EF} by 21 % in 2019, and B_{20} and B_{20A} reduced both cumulative CH_4 emissions and CH_{4EF} by 22% and 38 % in 2020 and 38% and 40 % in 2021 (Table S3; Table 2). The I×B interaction was significant in 2020 and 2021 due to B_{20} and B_{20A} reducing cumulative CH_4 emissions and CH_{4EF} by 22% and 39 % and 44% and 40 % under I_{CF}, while there was no significant difference under I_{AWD}. $I_{AWD}B_{20A}$ exhibited the lowest cumulative CH_4 emissions and CH_{4EF} across the three years, with reductions of 75 % in 2019, 85 % in 2020 and 89 % in 2021 compared to $I_{CF}B_0$ (Fig. 4a; Table 2).

3.6. Grain yield and water productivity

Grain yield was unaffected by the irrigation regime or the I×B interaction but was remarkably influenced by biochar across all three years (Fig. 4b). Compared to B_0, B_{20} decreased yield by 6 %, while B_{20A} was comparable in 2019, but B_{20} and B_{20A} improved yield by 5 % and 8 % in 2020 and 11 % and 12 % in 2021(Table S4).

There was a significant influence of irrigation regime on water use in the three years (Fig. 5a). Irrigation water use varied from 27.3

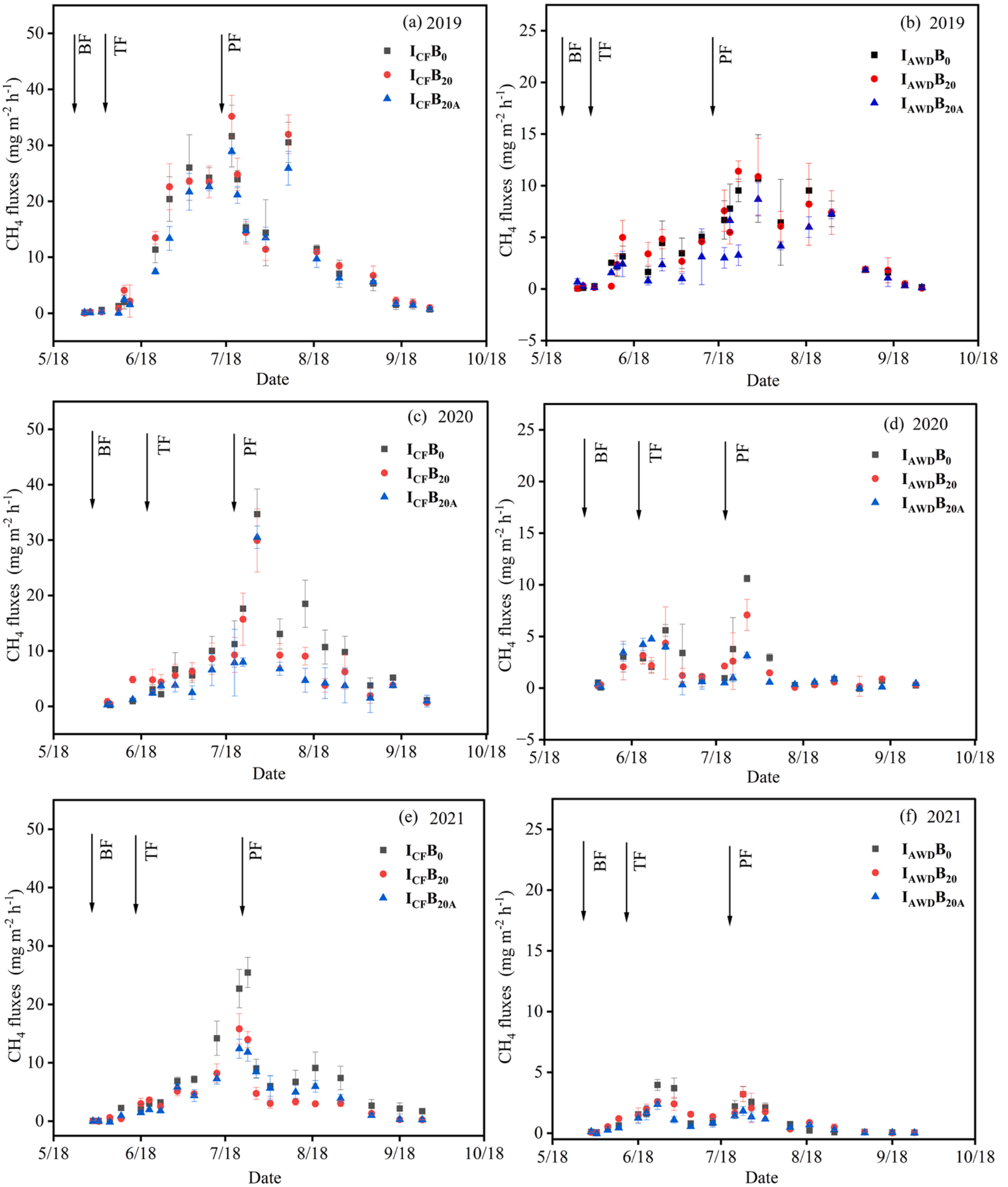

Fig. 3. Influence of irrigation regimes and biochar on CH_4 emission fluxes under six different treatments in 2019 (a, b), 2020 (c, d), and 2021 (e, f).

to 33.6 10^3 m^3 ha^{-1}, I_{AWD} reduced water use by 12 % in 2019, 11 % in 2020 and 10 % in 2021. Irrigation regime and biochar significantly impacted WUE across the three years (Fig. 5b). I_{AWD} significantly increased WUE by 13 % in 2019, 19 % in 2020 and 10 % in 2021, respectively. B_{20} only improved WUE by 5 % in 2020 and 15 % in 2021, however, B_{20A} remarkably increased WUE by 5 % in 2019, 8 % in 2020 and 15 % in 2021 (Table S7).

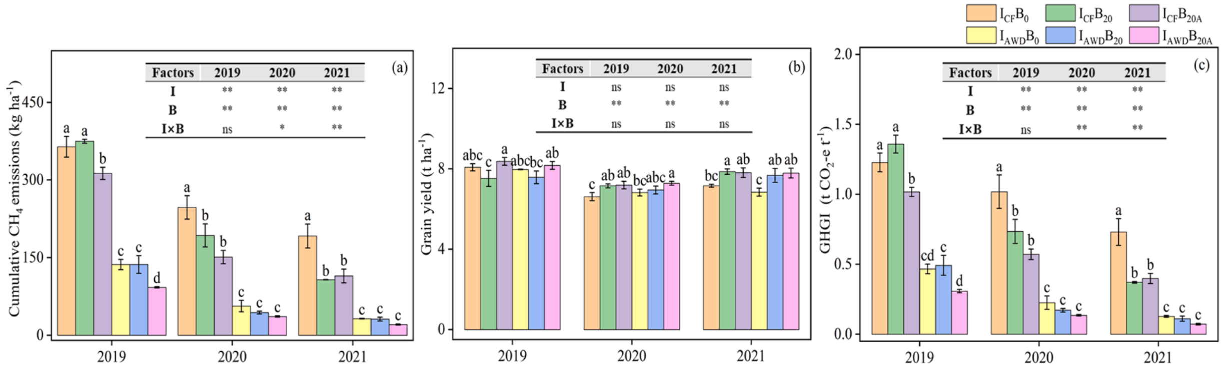

Fig. 4. Influence of irrigation regimes and biochar on cumulative CH_4 emissions during the growth season (a), grain yield (b) and GHGI (c) from 2019 to 2021. I: irrigation regime, B: biochar. B_0 represents no biochar, B_{20} and B_{20A} represent fresh biochar and acid modified biochar at 20 t ha^{-1} rate. * *: $P < 0.01$; * : $P < 0.05$; ns: no significant.

Table 2
Means and ANOVAs for CH_4 emission factors (CH_{4EF}) from 2019 to 2021 during rice growing season.

Treatments	CH_4 emission factors (kg CH_4 hm^{-2} d^{-1})		
	2019	2020	2021
I_{CF}	2.87 ± 0.25a	1.77 ± 0.41a	1.17 ± 0.36a
I_{AWD}	1.00 ± 0.20b	0.41 ± 0.09b	0.24 ± 0.05b
B_0	2.05 ± 1.03a	1.37 ± 0.95a	0.95 ± 0.75a
B_{20}	2.10 ± 1.07a	1.07 ± 0.75b	0.59 ± 0.35b
B_{20A}	1.66 ± 0.99b	0.84 ± 0.57b	0.57 ± 0.44b
$I_{CF}B_0$	2.98 ± 0.16a	2.22 ± 0.20a	1.62 ± 0.20a
$I_{CF}B_{20}$	3.07 ± 0.03a	1.74 ± 0.20b	0.91 ± 0.01b
$I_{CF}B_{20A}$	2.56 ± 0.10b	1.36 ± 0.12b	0.97 ± 0.11b
$I_{AWD}B_0$	1.12 ± 0.08c	0.51 ± 0.10c	0.27 ± 0.01c
$I_{AWD}B_{20}$	1.12 ± 0.14c	0.39 ± 0.02c	0.26 ± 0.03c
$I_{AWD}B_{20A}$	0.76 ± 0.01d	0.33 ± 0.01c	0.17 ± 0.01c
ANOVAs			
I	* *	* *	* *
B	* *	* *	* *
I×B	ns	*	* *

Means followed by different letters within the same column were notably different at $P < 0.05$. "* *", "* " and "ns" mean significance at $P < 0.01$, $P < 0.05$ and no significance. I: irrigation regime, B: biochar incorporation.

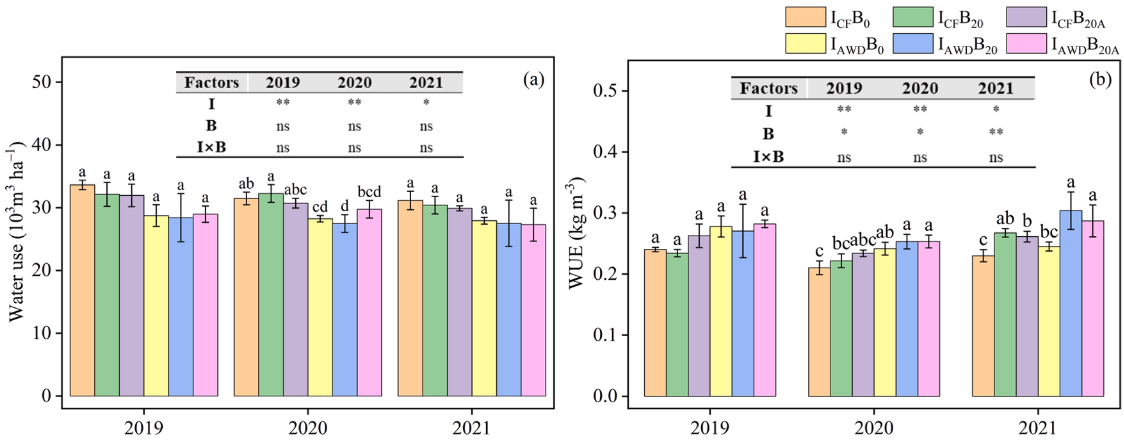

Fig. 5. Influence of irrigation regimes and biochar incorporation on water use (a) and WUE (b) from 2019 to 2021. I: irrigation regime, B: biochar. B_0 represents no biochar, B_{20} and B_{20A} represent fresh biochar and acid modified biochar at 20 t ha^{-1} rate. "* *", "* " and "ns" mean significance at $P < 0.01$, $P < 0.05$ and no significance.

3.7. Greenhouse gas emission intensity (GHGI)

GHGI was remarkably influenced by irrigation regime, biochar incorporation, and their interaction (except in 2019) over the three years (Fig. 4c). GHGI under I_{AWD} decreased by 65 %, 77 % and 79 % in 2019, 2020 and 2021, respectively. Compared to B_0, B_{20} decreased GHGI by 27 % in 2020 and 44 % in 2021, but B_{20A} reduced GHGI over the three years, being with 22 %, 43 % and 45 % in 2019, 2020 and 2021, respectively. (Table S4). The I×B interaction was significant in 2020 and 2021 because of B_{20} and B_{20A} reducing cumulative CH_4 emissions by 28% and 44 % and 49% and 45 % under I_{CF}, while there was no significant difference under I_{AWD}. $I_{AWD}B_{20A}$ exhibited the lowest GHGI over the three years, which was 75 %, 87 % and 90 % lower than $I_{CF}B_0$ in 2019, 2020, and 2021, respectively (Fig. 4c).

3.8. Path analysis between CH_4 emissions, GHGI and related factors

Path analysis results showed CH_4 emissions were remarkably and positively influenced by soil temperature (path coefficient, 0.39) and yield (0.24), and negatively affected by soil Eh (-0.66), NO_3^- (-0.49), SOC (-0.61), RD (-0.37), RLD (-0.28) (Fig. 6a). Among these factors, Eh and SOC were the most important factors affecting on CH_4 emissions, with the direct path coefficient of 0.72 and 0.50, respectively (Fig. 6b; Table 3). Chord diagram showed the extent to which soil factors (Eh, SOC and NO_3^-) and plant factors (RLD and RD) significantly influence CH_4 and GHGI emissions. As CH_4 is the main contributor to GHGI, all factors have the same rule of contribution to both CH_4 and GHGI emissions, and the degree of influence was as follows: soil Eh > SOC > RLD > RD > NO_3^- > Yield (Fig. 6b).

4. Discussion

4.1. Impact of biochar and AWD irrigation on CH_4 emissions

CH_4 emissions from soil include CH_4 production, oxidation and transport processes (Lee et al., 2023). CH_4 production and oxidation are very closely related to soil moisture. This study observed that CH_4 emission fluxes were generally lower under I_{AWD} (-0.05–11.40 mg m^{-2} h^{-1}) compared to I_{CF} (-0.16–35.17 mg m^{-2} h^{-1}) (Fig. 3). I_{AWD} decreased both CH_4 emissions and CH_{4EF} by 65–80 % over the three years (Table 2). From the perspective of influencing soil physical properties, there are three main reasons for this finding: 1) I_{AWD} improves soil aeration, promotes soil aerobic conditions, reduces methanogenic activity and inhibits methane production (Loaiza et al., 2024); 2) I_{AWD} can significantly increase soil Eh (Table 1), making the formation of an anaerobic environment difficult and stimulating methane oxidation. Meanwhile, I_{AWD} increases sulphate concentration and stimulates sulphate-reducing bacterial colonies to inhibit methane production (Souza et al., 2021); 3) I_{AWD} produces more inorganic nitrogen, providing a better nitrogen source for methanotrophs to act as a substrate for root oxidation, thereby reducing methane production. In our study, I_{AWD} soils can generate more NO_3^--N (Table 1) to serve as a substrate for CH_4 oxidation in the rhizosphere, thereby reducing CH_4 emissions. Path analysis further indicated that soil Eh was negatively correlated with CH_4 emissions and had the largest effect, with a direct path coefficient (0.72) (Fig. 6b; Table 3). However, our study demonstrated that I_{AWD} did not significantly affect rice root growth,

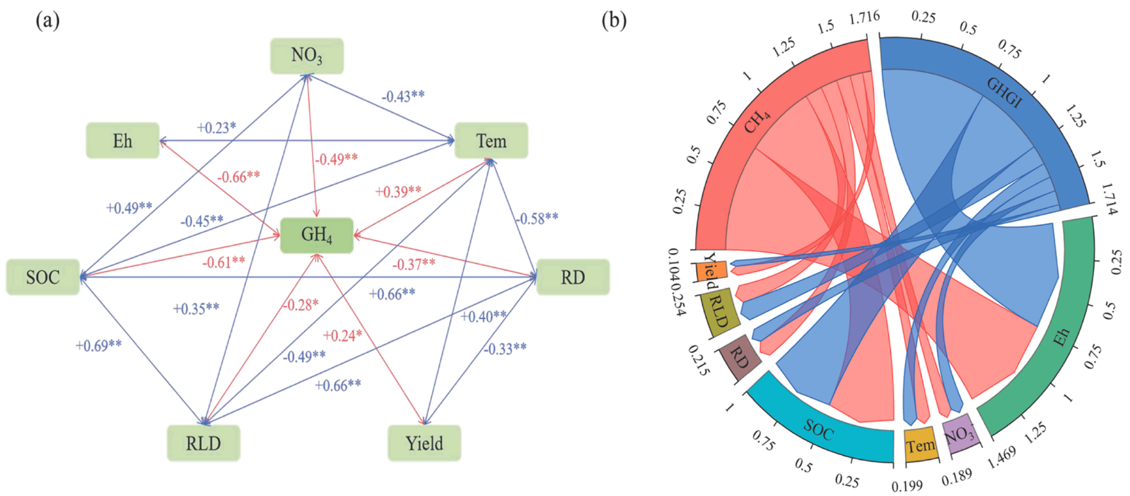

Fig. 6. Path analysis between CH_4 emissions and significantly related factors, including Eh, NO_3^-, Tem, SOC, RD, RLD and Yield (a). Red line represents correlation coefficient to CH_4 emissions. Blue line represents correlation coefficient among the related factors. "+ " and "-" mean positive and negative correlations. "* *" and "* " mean significance at $P < 0.01$ and $P < 0.05$. Chord diagram (b) indicates the magnitude of the effect between related factors on methane (red arrows) and GHGI (blue arrows), with thicker arrows indicating a greater effect and thinner arrows indicating a lesser effect.

Table 3
Path analysis between related factors and CH_4 emissions.

Related factors	Correlation coefficient with Y	Direct path coefficient	Indirect path coefficient												
			X_1-Y	X_2-Y	X_3-Y	X_4-Y	X_5-Y	X_6-Y	X_7-Y	X_8-Y	X_9-Y	X_{10}-Y	X_{11}-Y	X_{12}-Y	X_{13}-Y
X_1	−0.66	0.72		0.16	0.05	0.29	0.17	0.08	0.24	−0.13	−0.04	−0.07	−0.14	0.04	−0.01
X_2	0.06	0.08	0.02		0.01	0.02	0.04	0	0.04	0.02	0.01	−0.03	−0.01	0.04	0.06
X_3	−0.49	0.09	0.01	0.01		−0.04	−0.04	0.04	−0.01	0.03	0.02	0.01	0.03	0	0.01
X_4	0.22	0.26	0.1	0.08	−0.1		0.19	−0.07	0.14	−0.06	−0.02	−0.11	−0.14	−0.01	0.04
X_5	0.39	0.1	0.02	0.05	−0.04	0.07		−0.04	0.04	−0.02	−0.02	−0.06	−0.05	0	0.04
X_6	−0.61	0.5	0.05	0	0.25	−0.14	−0.22		0.01	0.26	0.31	0.33	0.34	0.26	−0.01
X_7	0.02	0.04	0.01	0.02	0	0.02	0.02	0		0.01	0	−0.01	−0.01	0.02	0.02
X_8	−0.12	0.04	−0.01	0.01	0.01	−0.01	−0.01	0.02	0.01		0.02	0.01	0.02	0.02	0.01
X_9	−0.15	0.13	−0.01	0.01	0.02	−0.01	−0.03	0.08	0.01	0.05		0.07	0.06	0.06	0.03
X_{10}	−0.37	0.12	−0.01	−0.04	0.01	−0.05	−0.07	0.08	−0.03	0.03	0.06		0.08	0.05	−0.04
X_{11}	−0.28	0.12	−0.02	−0.01	0.04	−0.07	−0.06	0.08	−0.02	0.05	0.06	0.08		0.05	0.01
X_{12}	−0.1	0.14	0.01	0.06	0	0	0.01	0.07	0.06	0.08	0.07	0.05	0.06		0.07
X_{13}	0.24	0.06	0	0.05	0.01	0.01	0.03	0	0.03	0.02	0.01	−0.02	0	0.03	

Y represent CH_4 emissions, X_1, X_2, X_3, X_4, X_5, X_6, X_7, X_8, X_9, X_{10}, X_{11}, X_{12}, X_{13} represent Eh, NH_4^+, NO_3^-, pH, Tem, SOC, CEC, C/N, RDW, RD, RLD and DMA and Yield, respectively.

potentially due to constrained root space from high local sowing density (Arai et al., 2021). In addition, I_{AWD} can cause organic carbon loss, decrease soil fertility and lead to reduced crop yields (Fertitta-Roberts et al., 2019; Livsey et al., 2019). However, it was worth noting that I_{AWD} has no significant effect on SOC in this study. First, the experimental site in Liaohe Plain has a higher water conductivity characteristic typical of fluvial alluvial sediments, indicating that I_{AWD} reduces water infiltration and consequently the loss of organic and soluble carbon. Secondly, the effect of irrigation regimes on SOC in the short term is not as significant as in the long term. Therefore, it is still worth exploring effective strategies to increase soil carbon and improve soil fertility while ensuring water savings and emission reductions.

Biochar can alter soil physical and chemical properties, thereby directly or indirectly influencing CH_4 production and oxidation (Zhao et al., 2024). Current research on the impacts of biochar on CH_4 emissions remains inconsistent, with studies reporting decreases (Dai et al., 2024), increases (Chen et al., 2020) or no effect (Liu et al., 2016) in rice fields. These inconsistencies can be attributed to differences in soil types, biochar types and application rates. In this study, we found that B_{20} increased CH_4 emissions in the first year, whereas B_{20A} significantly inhibited both CH_4 and CH_{4EF} emissions by 21 % (Table S3; Table 2). This result was due to soil pH increased by 0.23 units and stimulated the activity of methanogenic bacteria, thus promoting CH_4 emissions (Ribas et al., 2019). In addition, soil temperature also plays an important role in affecting the activity of methanogens (Dai et al., 2024). Soil temperature improved (0.34°C) due to biochar incorporation in the first year, and CH_4 emission was positively correlated with soil temperature (Fig. 6), and the increase in temperature stimulated methane production. However, acid modified biochar had no effect in soil temperature and enhanced acid functional group and oxygen-containing functional groups, such as -COOH and -OH (Table 1; Fig. S4c), which enhanced the hydrophilicity and inhibited the tendency of biochar to elevate pH (3 % lower than B_{20}) and temperature (0.45°C lower than B_{20}), thereby inhibiting the activity of methanogenesis and reducing CH_4 emissions (Gong et al., 2024). Therefore, acid modified alleviated biochar-induced initial methane emissions and yield decrease.

In the following two years, we found that both B_{20} (22 %-38 %) and B_{20A} (38 %-40 %) effectively reduced CH_4 emissions, and that acidified biochar had a greater reduction potential (Table S3; Table 2). Firstly, the incorporation of biochar will inevitably affect the level of soil organic carbon, including unstable and inert carbon, and then the reaction substrate produced by methane (Han et al., 2020). B_{20A} had a lower carbon content when compared with B_{20} (Table S2), which may be caused by the large amount of water washing during the preparation process, reducing the unstable carbon. Both B_{20} and B_{20A} increased SOC, but B_{20A} had a greater improvement (27 %~44 %) (Table 1). We speculate that B_{20A} can decompose or convert unstable organic C into stable SOC to suppress the availability of the substrate for CH_4 production and enhance soil fertility by decreasing microbially available substrates (Gong et al., 2024; Wu et al., 2019). Path analysis also showed that SOC was negatively correlated with CH_4 emissions and was the second most important factor affecting CH_4 emissions (Fig. 6a, b), with a direct path coefficient (0.50) (Fig. 6b; Table 3). Secondly, root growth is also an important factor in regulating CH_4 emissions (Chen et al., 2019). Biochar provided a loose and porous growth environment for roots, which was conducive to water and nutrient retention and improved root growth (Zhang et al., 2023), significantly increasing RDW, RD and RLD (Fig. 2b-d). The negative correlation between CH_4 emissions, RD and RLD (Fig. 6a). The improved root morphology provided favorable conditions for microorganisms and increased the abundance and activity of methanoxobacteria. CH_4 oxidation enhanced and reduced CH_4 emission factors. Whereas, it is worth noting that acidified biochar has a higher emission reduction potential than fresh biochar, which may be due to its greater stability and higher C/N (Table S2; Fig. S4), increased specific surface area and pore size after acidifying water washing, which increases soil aeration and provides a more favorable habitat for methanotrophic bacteria (Gong et al., 2024; Lin et al., 2022; Wen et al., 2021), thereby increasing the number and activity of methanogens and contributing to CH_4 oxidation. Sriphirom et al. (2020) recommended that biochar combined with I_{AWD} mitigated CH_4 emissions, but our findings further revealed that $I_{AWD}B_{20A}$ was the best measure for decreasing methane emissions and enhancing SOC and rice yield (Fig. 4; Table 2), realizing low-carbon production under alternate wetting and drying rice paddy.

4.2. Impact of biochar and AWD irrigation on water productivity

As a mainly agricultural country, China is increasingly facing the problem of water scarcity, especially agricultural water. To ensure grain yield and alleviate water scarcity, irrigation regimes in paddy fields have been targeted in recent years (Wang et al., 2020; Xu et al., 2015). I_{AWD} has been applied to high consumption crops such as paddy and has proven to be an effective measure to conserve water, maintain production and improve WUE (Pan et al., 2017; Wang et al., 2020). I_{AWD} reduced water consumption by 10–12 % and improved WUE by 10–19 % over the three years (Table S7). However, Carrijo et al. (2017) demonstrated that I_{AWD} reduced water consumption by 25.7 % and enhanced WUE by 24.2 %, with a higher water-saving capacity than our study. This was primarily due to the high rates of water percolation (17.6–31.1 10^3 m^3 ha^{-1}) and water consumption observed at our experimental site, which was formed by the alluvium of the Liaohe River watershed. Furthermore, water percolation accounted for 79–87 % of the total water input in the silty loam, resulting in a large amount of water waste (Han et al., 2023a). Thus, it is of great importance to seek a new method to combine with AWD irrigation to improve WUE and rice productivity in this area.

Biochar has been shown to induce the need for irrigation water demands and improve WUE in rice fields (Han et al., 2023a; Lehmann et al., 2015). Aller et al. (2017) discovered that WUE was affected by soil types and biochar age. Fresh and aged biochar reduced WUE in clay soils, but not in silty soils through soil column experiment. However, this study observed that B_{20} and B_{20A} increased WUE in the rice fields on the silty clay soil. First, biochar improved soil structure and increased the proportion of fine soil particles, thereby elevating soil water retention (Table S5). Second, biochar enhanced soil water-holding capacity due to its high surface area, porosity and ability to increase soil C stocks (Table 1), resulting in lower water consumption and higher WUE (Kang et al., 2022; Han et al., 2023a). Moreover, it was possibly due to the improved water-holding capacity and leaf photosynthesis (Zhou et al., 2018). Notably, B_{20} improved WUE only in 2020 and 2021, but not in 2019 (Fig. 5b; Table S7), which can be attributed to a lower yield in 2019. However, B_{20A} increased rice yield for three consecutive years. Acid modified biochar improved hydrophilicity due to an increase in surface carboxyl groups and other functional groups (Fig. S4c) and was more likely to form hydrogen bonds with highly negative surface oxygen. Concurrently, its adsorption ability increased (Bushra and Remya, 2024), resulting in a 5–15 % increase in WUE within three years (Fig. 5b; Table S7). This suggests that acid modified biochar has a greater water saving potential. Acid modified biochar combined with I_{AWD} achieved the highest WUE over three years (Fig. 5b), demonstrating its effectiveness in enhancing WUE and reducing water consumption, particularly in AWD rice fields.

4.3. Impact of biochar and AWD irrigation on yield and GHGI

Irrigation regimes had no significant impact on rice yield, but I_{AWD} saved 10–12 % of water consumption (Fig. 5b), indicating that I_{AWD} can effectively reduce water consumption without a reduction in yield. On the one hand, the sandy loam soil quality in this experiment could be drained quickly, and the short drainage time was conducive to maintaining the soil available water and providing roots with sufficient water, thus preventing drought-induced yield reductions. (Carrijo et al., 2018). On the other hand, it is possible that I_{AWD} increased soil permeability, provided O_2 for root growth, and promoted mineralization of soil organic matter, which ensured rice yield (Oo et al., 2018). I_{AWD} mitigated GHGI by 65–79 % over the three years, which was caused by the reduction of CH_4 emissions and CH_{4EF} under I_{AWD} (Table 2; Table S4). But the reduction in GHGI emissions in our study was greater than the 38.4 % reported by Ariani et al. (2022), probably due to this study did not consider the increase in N_2O emissions under I_{AWD}. Although GHGI emissions in paddy fields mainly depend on CH_4 emissions, N_2O emissions cannot be ignored (Loaiza et al., 2024). AWD reduces CH_4 emissions by 97 %, while N_2O emissions increase five times (Lagomarsino et al., 2016). In summary, our study suggests that rice production can be optimized through I_{AWD} to ensure stable rice yield and decrease water consumption while mitigating GHGI.

The response of grain yield to biochar varies with soil characteristics, biochar type, and its application time. (Gong et al., 2024; Liu et al., 2021). Raw biochar had an insignificant effect on soybean yield (Gong et al., 2024). Whereas, Zhou et al. (2018) observed a 5.49 % increase in yields with biochar, primarily due to improvements in soil nutrient availability and physical properties. The extent of yield enhancement and the persistence of these beneficial effects are significantly influenced by soil fertility and biochar properties. (Kang et al., 2022; Liu et al., 2019). Major et al. (2010) observed that 20 $t \cdot ha^{-1}$ biochar had no remarkable impact on maize yield in the initial year, while it consistently improved in subsequent years, this result was consistent with our finding. We found that both B_{20} and B_{20A} enhanced yield by 5 % and 8 % in 2020, 11 % and 12 % in 2021, and B_{20A} showed better positive impacts, especially in the first year, B_{20} decreased yield but B_{20A} maintained stable yield (Table S4). The initial yield decline was attributable to an elevated soil pH (4 % higher) from biochar, causing a liming effect. However, FE-SEM images revealed that the surface of B_{20A} was smoother than B_{20} (Fig. S4a-b), indicating that it can effectively remove excess impurities and ash and inhibit the initial lime effect (Wang et al., 2024). Subsequent yield improvements resulted from the stabilization of soil pH and enhanced nutrient availability, including elevated levels of inorganic nitrogen and SOC from biochar incorporation (Table 1), which boosted soil fertility. However, B_{20A} enhanced carboxyl groups (-COOH), one of the main acidic groups (Figure S4), which effectively lowered the pH and inhibited the initial liming effect of biochar. Additionally, post-harvest C/N significantly improved with biochar incorporation (Fig. 1d-f), especially under B_{20A}, enhancing soil fertility and rice yield (Xie et al., 2021). We further found that the greater yield response to acid modified biochar was attributed its greater increase in potassium available at the soil surface, an enhancement of C=O sorption peak, thereby increasing soil CEC. Generally, C=O is usually positively correlated with CEC (Liu et al., 2022). CEC is also an important factor in measuring the level of soil fertility. In this study, B_{20A} significantly increased post-harvest CEC in three growing seasons (Fig. 1a-c), demonstrating that B_{20A} effectively improved soil fertility and contributed to rice production, which was consistent with Gong et al. (2024). In addition, the higher specific surface area and SOC of B_{20A} and the higher abundance of functional genes involved in carbon decomposition and carbon sequestration are conducive to the improvement in nutrient effectiveness and acceleration in soil cycling, which are also responsible for the increase in rice yield (Gong et al., 2024; Joseph et al., 2021). In addition, SEM showed that there were many irregular particles on the surface of B_{20A}, which increased surface porosity and made it have more active adsorption sites. Raman spectra also showed that ID/IG reflected biochar defects, B_{20A} was higher than B_{20} (Fig. S4d), indicating that B_{20A} contained more defects and provided the most active site, which was conducive to nutrient retention and crop yield improvement (Gong et al., 2024; Li et al., 2025).

GHGI emission is closely related to production and CH_4 emission. Our findings indicated that B_{20} reduced GHGI in 2020 and 2021, but in the first year the reduction effect was not significant and there was even a risk of increasing emissions. However, B_{20A} reduced GHGI for three consecutive years, effectively reducing GHG emissions from rice fields (Table S4). Firstly, acid modified biochar increased rice yields for three consecutive years, while B_{20} reduced yields in the first year due to the lime effect. Secondly, it was also mainly influenced by CH_4 emission, as B_{20A} enhanced acidic functional groups (Fig. S4c), which offset the adverse effects resulting from the pH increase. Thus, B_{20A} exhibited superior inhibition of CH_4 emission during the first year, thereby reducing the GHGI. We further found that $I_{AWD}B_{20A}$ emitted the lowest GHGI, 75–90 % lower than $I_{CF}B_0$ over the three years. Overall, combining acid modified biochar with I_{AWD} is the best treatment in GHG emission reduction yield enhancement in paddy fields.

5. Practical applications and prospects

Converting rice straw into biochar and its application to the soil not only solves the problem of straw waste and reduces carbon emissions but also realizes "taking from the field and applying to the field", which is conducive to promoting the green, low-carbon and sustainable development of the rice field. However, variations in biochar preparation technology, types, and durations, as well as differences in regional conditions, climates, and soil types, can lead to diverse outcomes regarding the impact of biochar on GHG emissions and rice growth (Shaukat et al., 2019). This study conducted a 3-yr in situ field experiment in cold areas of northern China, and found that biochar reduced CH_4 emissions, promoted soil fertility and rice growth. Acid modified biochar showed a better potential performance, alleviating biochar-induced initial CH_4 emissions and yield decrease, especially under I_{AWD}. In Northeast China, the main rice production base, where water shortage is increasingly serious, I_{AWD} can effectively reduce the irrigation water consumption, and the application of acid modified biochar to I_{AWD} paddy fields has great potential for emission reduction and yield increase, as well as has a good application prospect. Therefore, in the future, it is of great significance to consider promoting research in other regions of China and major rice-producing countries to achieve low-carbon production and United Nations Sustainable Development Goals (UN SDGs), mitigate the global greenhouse effect, and increase rice production to solve the food security problem caused by the increasing world population.

6. Conclusions

B_{20} reduced CH_4 emissions and increased grain yield in the 2^{nd} and 3^{rd} year after its initial application, but decreased grain yield and tended to increase CH_4 emissions in the 1^{st} year. B_{20A} addressed these issues, which consistently inhibited CH_4 emissions and did not alter grain yield throughout the three years. The positive effect under B_{20A} was primarily attributed to enhanced acidic and oxygenated functional group effectively lowered its pH and suppressed the liming effect. Among six treatments, $I_{AWD}B_{20A}$ had the highest yield and the lowest CH_4 emissions and GHGI in the three years. Overall, engineered biochar with acid modification alleviates biochar-induced initial methane emissions and yield decrease, realizing low-carbon production under AWD rice paddy. It is of great significance for realizing low carbon emissions and promoting rice sustainable development. Given the high cost of biochar, further investigation of its effects on net ecosystem economic benefits in I_{AWD} paddy is warranted.

Declaration

The authors confirm that they have no financial or personal conflicts of interest that could have affected the conduct or outcomes of the research presented in this study.

CRediT authorship contribution statement

Chen Taotao: Writing – review & editing, Supervision, Project administration, Funding acquisition, Conceptualization. **Liu Chang:** Writing – review & editing, Writing – original draft, Investigation, Formal analysis, Conceptualization. **Ok Yong Sik:** Writing – review & editing, Conceptualization. **Chi Daocai:** Supervision, Project administration, Funding acquisition. **Meng Jun:** Supervision, Resources. **Yi Benji:** Visualization, Investigation. **Han Hongwei:** Investigation, Data curation. **Zhang Feng:** Software, Investigation.

Acknowledgements

This research was funded by the National Nature Science Foundation of China (52379043), the Liaoning Province Applied Basic Research Program for Cultivating Young Science and Technology Talent (2023030237-JH2/1016), the China Postdoctoral Science Foundation Funded Project (2019M661129), and the Liaoning Revitalization Talents Program (XLYC1902064). Chang Liu acknowledges the support from the China Scholarship Council and Korea University for hosting her visiting research. This research was supported by Basic Science Research Program through the National Research Foundation of Korea (NRF) funded by the Ministry of Education (NRF-2021RA6A1A10045235).This work was supported by the Technology Innovation Program (00432915) funded By the Ministry of Trade, Industry & Energy (MOTIE, Korea).

Declaration of Competing Interest

The authors declare that they have no competing financial interests or personal relationships that might have influenced the experiment reported in this paper.

Appendix A. Supporting information

Supplementary data associated with this article can be found in the online version at doi:10.1016/j.eti.2025.104133.

Data Availability

Data are included in the supplimentary materials

References

Ai, B., Sheng, Z., Zheng, L., Shang, W., 2015. Collectable Amounts of Straw Resources and Their Distribution in China, in: Proceedings of the International Conference on Advances in Energy, Environment and Chemical Engineering. Presented at the International Conference on Advances in Energy, Environment and Chemical Engineering, Atlantis Press, Changska, China. https://doi.org/10.2991/aeece-15.2015.89.

Aller, D., Rathke, S., Laird, D., Cruse, R., Hatfield, J., 2017. Impacts of fresh and aged biochars on plant available water and water use efficiency. Geoderma 307, 114–121. https://doi.org/10.1016/j.geoderma.2017.08.007.

Arai, H., Hosen, Y., Chiem, N.H., Inubushi, K., 2021. Alternate wetting and drying enhanced the yield of a triple-cropping rice paddy of the Mekong Delta. Soil Sci. Plant Nutr. 67, 493–506. https://doi.org/10.1080/00380768.2021.1929463.

Ariani, M., Hanudin, E., Haryono, E., 2022. The effect of contrasting soil textures on the efficiency of alternate wetting-drying to reduce water use and global warming potential. Agric. Water Manag. 274, 107970. https://doi.org/10.1016/j.agwat.2022.107970.

Ashworth, D.J., Schmidt, M.P., Ibekwe, A.M., 2023. Performance of acid- and base-modified biochars for the removal of antibiotics from water under dynamic conditions. J. Environ. Chem. Eng. 11, 111616. https://doi.org/10.1016/j.jece.2023.111616.

Berhane, M., Xu, M., Liang, Z., Shi, J., Wei, G., Tian, X., 2020. Effects of long-term straw return on soil organic carbon storage and sequestration rate in North China upland crops: a meta-analysis. Glob. Change Biol. 26, 2686–2701. https://doi.org/10.1111/gcb.15018.

Boguta, P., Sokołowska, Z., Skic, K., Tomczyk, A., 2019. Chemically engineered biochar – Effect of concentration and type of modifier on sorption and structural properties of biochar from wood waste. Fuel 256, 115893. https://doi.org/10.1016/j.fuel.2019.115893.

Bushra, B., Remya, N., 2024. Biochar from pyrolysis of rice husk biomass—characteristics, modification and environmental application. Biomass-.-. Conv. Bioref. 14, 5759–5770. https://doi.org/10.1007/s13399-020-01092-3.

Carrijo, D.R., Lundy, M.E., Linquist, B.A., 2017. Rice yields and water use under alternate wetting and drying irrigation: a meta-analysis. Field Crops Res. 203, 173–180. https://doi.org/10.1016/j.fcr.2016.12.002.

Carrijo, D.R., Akbar, N., Reis, A.F.B., Li, C., Gaudin, A.C.M., Parikh, S.J., Green, P.G., Linquist, B.A., 2018. Impacts of variable soil drying in alternate wetting and drying rice systems on yields, grain arsenic concentration and soil moisture dynamics. Field Crops Res. 222, 101–110. https://doi.org/10.1016/j.fcr.2018.02.026.

Chen, J., Zhou, J., Zheng, W., Leng, S., Ai, Z., Zhang, W., Yang, Z., Yang, J., Xu, Z., Cao, J., Zhang, M., Leng, L., Li, H., 2024. A complete review on the oxygen-containing functional groups of biochar: formation mechanisms, detection methods, engineering, and applications. Sci. Total Environ. 946, 174081. https://doi.org/10.1016/j.scitotenv.2024.174081.

Chen, T., Liu, C., Zhang, F., Han, H., Wang, Z., Yi, B., Tang, L., Meng, J., Chi, D., Wilson, L.T., Chen, W., 2022. Acid-modified biochar increases grain yield and reduces reactive gaseous N losses and N-related global warming potential in alternate wetting and drying paddy production system. J. Clean. Prod. 377, 134451. https://doi.org/10.1016/j.jclepro.2022.134451.

Chen, X., Zhu, H., Bañuelos, G., Shutes, B., Yan, B., Cheng, R., 2020. Biochar reduces nitrous oxide but increases methane emissions in batch wetland mesocosms. Chem. Eng. J. 392, 124842. https://doi.org/10.1016/j.cej.2020.124842.

Chen, Y., Li, S., Zhang, Y., Li, T., Ge, H., Xia, S., Gu, J., Zhang, H., Lü, B., Wu, X., Wang, Z., Yang, J., Zhang, J., Liu, L., 2019. Rice root morphological and physiological traits interaction with rhizosphere soil and its effect on methane emissions in paddy fields. Soil Biol. Biochem. 129, 191–200. https://doi.org/10.1016/j.soilbio.2018.11.015.

Chu, G., Chen, T., Chen, S., Xu, C., Wang, D., Zhang, X., 2018. Agronomic performance of drought-resistance rice cultivars grown under alternate wetting and drying irrigation management in southeast China. Crop J. 6, 482–494. https://doi.org/10.1016/j.cj.2018.04.005.

Dai, W., Bao, Z., Meng, J., Chen, T., Zhang, W., Chen, Y., Lin, L., Su, X., Jiang, X., 2024. Biochar incorporation increases grain yield, net ecosystem CO_2 exchange, and decreases CH_4 emissions in an alternate wetting and drying paddy ecosystem. Environ. Technol. Innov. 34, 103577. https://doi.org/10.1016/j.eti.2024.103577.

Ding, H., Jiang, Y., Cao, C., 2021. Deep rice root systems reduce methane emissions in rice paddies. Plant Soil 468, 337–352. https://doi.org/10.1007/s11104-021-05118-1.

Duan, P., Zhang, X., Zhang, Q., Wu, Z., Xiong, Z., 2018. Field-aged biochar stimulated N_2O production from greenhouse vegetable production soils by nitrification and denitrification. Sci. Total Environ. 642, 1303–1310. https://doi.org/10.1016/j.scitotenv.2018.06.166.

Fertitta-Roberts, C., Oikawa, P.Y., Darrel Jenerette, G., 2019. Evaluating the GHG mitigation-potential of alternate wetting and drying in rice through life cycle assessment. Sci. Total Environ. 653, 1343–1353. https://doi.org/10.1016/j.scitotenv.2018.10.327.

Forster, P., Storelvmo, T., Armour, K., Collins, W., Dufresne, J.-L., Frame, D., Lunt, D., Mauritsen, T., Palmer, M., Watanabe, M., Wild, M., Zhang, H., 2021. Chapter 7: The Earth's energy budget, climate feedbacks, and climate sensitivity. https://doi.org/10.25455/wgtn.16869671.v1.

Godwin, P.M., Pan, Y., Xiao, H., Afzal, M.T., 2019. Progress in preparation and application of modified biochar for improving heavy metal ion removal from wastewater. J. Bioresour. Bioprod. 4, 31–42. https://doi.org/10.21967/jbb.v4i1.180.

Gong, Y., Hou, R., Fu, Q., Li, T., Wang, J., Su, Z., Shen, W., Zhou, W., Wang, Y., Li, M., 2024. Modified biochar reduces the greenhouse gas emission intensity and enhances the net ecosystem economic budget in black soil soybean fields. Soil Tillage Res. 237, 105978. https://doi.org/10.1016/j.still.2023.105978.

Han, H., Chen, T., Liu, C., Zhang, F., Sun, Y., Bai, Y., Meng, J., Chi, D., Chen, W., 2023a. Effects of acid modified biochar on potassium uptake, leaching and balance in an alternate wetting and drying paddy ecosystem. Sci. Total Environ. 900, 166344. https://doi.org/10.1016/j.scitotenv.2023.166344.

Han, L., Sun, K., Yang, Y., Xia, X., Li, F., Yang, Z., Xing, B., 2020. Biochar's stability and effect on the content, composition and turnover of soil organic carbon. Geoderma 364, 114184. https://doi.org/10.1016/j.geoderma.2020.114184.

Han, Y., Zhang, Zhongxue, Li, T., Chen, P., Nie, T., Zhang, Zuohe, Du, S., 2023b. Straw return alleviates the greenhouse effect of paddy fields by increasing soil organic carbon sequestration under water-saving irrigation. Agric. Water Manag. 287, 108434. https://doi.org/10.1016/j.agwat.2023.108434.

He, T., Yuan, J., Luo, J., Lindsey, S., Xiang, J., Lin, Y., Liu, D., Chen, Z., Ding, W., 2020. Combined application of biochar with urease and nitrification inhibitors have synergistic effects on mitigating CH_4 emissions in rice field: a three-year study. Sci. Total Environ. 743, 140500. https://doi.org/10.1016/j.scitotenv.2020.140500.

He, X., Hong, Z., Shi, R., Cui, J., Lai, H., Lu, H., Xu, R., 2022. The effects of H_2O_2- and HNO_3/H_2SO_4-modified biochars on the resistance of acid paddy soil to acidification. Environ. Pollut. 293, 118588. https://doi.org/10.1016/j.envpol.2021.118588.

Joseph, S., Cowie, A.L., Van Zwieten, L., Bolan, N., Budai, A., Buss, W., Cayuela, M.L., Graber, E.R., Ippolito, J.A., Kuzyakov, Y., Luo, Y., Ok, Y.S., Palansooriya, K.N., Shepherd, J., Stephens, S., Weng, Z., (Han), Lehmann, J., 2021. How biochar works, and when it doesn't: a review of mechanisms controlling soil and plant responses to biochar. GCB Bioenergy 13, 1731–1764. https://doi.org/10.1111/gcbb.12885.

Kang, M.W., Yibeltal, M., Kim, Y.H., Oh, S.J., Lee, J.C., Kwon, E.E., Lee, S.S., 2022. Enhancement of soil physical properties and soil water retention with biochar-based soil amendments. Sci. Total Environ. 836, 155746. https://doi.org/10.1016/j.scitotenv.2022.155746.

Kasera, N., Augoustides, V., Kolar, P., Hall, S., Vicente, B., 2022. Effect of surface modification by oxygen-enriched chemicals on the surface properties of pine bark biochars. Processes 10, 2136. https://doi.org/10.3390/pr10102136.

Lagomarsino, A., Agnelli, A.E., Linquist, B., Adviento-borbe, M.A., Agnelli, A., Gavina, G., Ravaglia, S., Ferrara, R.M., 2016. Alternate wetting and drying of rice reduced CH_4 emissions but triggered N_2O peaks in a clayey soil of central Italy. Pedosphere 26, 533–548. https://doi.org/10.1016/S1002-0160(15)60063-7.

Lee, J., Oh, Y., Lee, S.T., Seo, Y.O., Yun, J., Yang, Y., Kim, J., Zhuang, Q., Kang, H., 2023. Soil organic carbon is a key determinant of CH_4 sink in global forest soils. Nat. Commun. 14, 3110. https://doi.org/10.1038/s41467-023-38905-8.

Lehmann, J., Kuzyakov, Y., Pan, G., Ok, Y.S., 2015. Biochars and the plant-soil interface. Plant Soil 395, 1–5. https://doi.org/10.1007/s11104-015-2658-3.

Li, J., Li, Y., Wan, Y., Wang, B., Cai, W., Qin, X., Zhou, Z., Wang, X., Yuan, J., Deng, Q., 2024. Annual greenhouse gas emissions from a rice paddy with different water-nitrogen management strategies in Central China. Soil Tillage Res. 235, 105906. https://doi.org/10.1016/j.still.2023.105906.

Li, L., Zhao, J., Zhao, X., Zhou, Z., Jing, G., 2025. Insight into the mechanism of peracetic acid activation by corn straw-derived biochar as efficient green activator mediating electron transfer: crucial role of carbonyl functional group. Sep. Purif. Technol. 354, 129005. https://doi.org/10.1016/j.seppur.2024.129005.

Li, Y., Zheng, J., Wu, Q., Gong, X., Zhang, Z., Chen, Y., Chen, T., Siddique, K.H.M., Chi, D., 2022. Zeolite increases paddy soil potassium fixation, partial factor productivity, and potassium balance under alternate wetting and drying irrigation. Agric. Water Manag. 260, 107294. https://doi.org/10.1016/j.agwat.2021.107294.

Lin, X., Wang, N., Li, F., Yan, B., Pan, J., Jiang, S., Peng, H., Chen, A., Wu, G., Zhang, J., Zhang, L., Huang, H., Luo, L., 2022. Evaluation of the synergistic effects of biochar and biogas residue on CO_2 and CH_4 emission, functional genes, and enzyme activity during straw composting. Bioresour. Technol. 360, 127608. https://doi.org/10.1016/j.biortech.2022.127608.

Liu, J., Huang, X., Jiang, H., Chen, H., 2021. Sustaining yield and mitigating methane emissions from rice production with plastic film mulching technique. Agric. Water Manag. 245, 106667. https://doi.org/10.1016/j.agwat.2020.106667.

Liu, Q., Liu, B., Ambus, P., Zhang, Y., Hansen, V., Lin, Z., Shen, D., Liu, G., Bei, Q., Zhu, J., Wang, X., Ma, J., Lin, X., Yu, Y., Zhu, C., Xie, Z., 2016. Carbon footprint of rice production under biochar amendment – a case study in a Chinese rice cropping system. GCB Bioenergy 8, 148–159. https://doi.org/10.1111/gcbb.12248.

Liu, Q., Zhong, L., Hu, Y., Fu, L., Hu, X., Gu, Y., Xie, Q., Liang, F., Liu, Qi, Lu, Y., 2022. Effects of modified biochars on the shifts of short-chain fatty acid profile, iron reduction, and bacterial community in paddy soil. FEMS Microbiol. Ecol. 98, 1–10. https://doi.org/10.1093/femsec/fiac131.

Liu, R., Hu, Y., Zhan, X., Zhong, J., Zhao, P., Feng, H., Dong, Q., Siddique, K.H.M., 2024. The response of crop yield, carbon sequestration, and global warming potential to straw and biochar applications: a meta-analysis. Sci. Total Environ. 907, 167884. https://doi.org/10.1016/j.scitotenv.2023.167884.

Liu, X., Zhou, J., Chi, Z., Zheng, Jufeng, Li, L., Zhang, X., Zheng, Jinwei, Cheng, K., Bian, R., Pan, G., 2019. Biochar provided limited benefits for rice yield and greenhouse gas mitigation six years following an amendment in a fertile rice paddy. CATENA 179, 20–28. https://doi.org/10.1016/j.catena.2019.03.033.

Livsey, J., Kätterer, T., Vico, G., Lyon, S.W., Lindborg, R., Scaini, A., Da, C.T., Manzoni, S., 2019. Do alternative irrigation strategies for rice cultivation decrease water footprints at the cost of long-term soil health. Environ. Res. Lett. 14, 074011. https://doi.org/10.1088/1748-9326/ab2108.

Loaiza, S., Verchot, L., Valencia, D., Guzmán, P., Amezquita, N., Garcés, G., Puentes, O., Trujillo, C., Chirinda, N., Pittelkow, C.M., 2024. Evaluating greenhouse gas mitigation through alternate wetting and drying irrigation in Colombian rice production. Agric., Ecosyst. Environ. 360, 108787. https://doi.org/10.1016/j.agee.2023.108787.

Major, J., Rondon, M., Molina, D., Riha, S.J., Lehmann, J., 2010. Maize yield and nutrition during 4 years after biochar application to a Colombian savanna oxisol. Plant Soil 333, 117–128. https://doi.org/10.1007/s11104-010-0327-0.

Nan, Q., Hu, S., Qin, Y., Wu, W., 2021. Methane oxidation activity inhibition via high amount aged biochar application in paddy soil. Sci. Total Environ. 796, 149050. https://doi.org/10.1016/j.scitotenv.2021.149050.

Nan, Q., Fang, C., Cheng, L., Hao, W., Wu, W., 2022. Elevation of NO_3^--N from biochar amendment facilitates mitigating paddy CH_4 emission stably over seven years. Environ. Pollut. 295, 118707. https://doi.org/10.1016/j.envpol.2021.118707.

Nikolaisen, M., Cornulier, T., Hillier, J., Smith, P., Albanito, F., Nayak, D., 2023. Methane emissions from rice paddies globally: a quantitative statistical review of controlling variables and modelling of emission factors. J. Clean. Prod. 409, 137245. https://doi.org/10.1016/j.jclepro.2023.137245.

Oo, A.Z., Sudo, S., Inubushi, K., Chellappan, U., Yamamoto, A., Ono, K., Mano, M., Hayashida, S., Koothan, V., Osawa, T., Terao, Y., Palanisamy, J., Palanisamy, E., Venkatachalam, R., 2018. Mitigation potential and yield-scaled global warming potential of early-season drainage from a rice paddy in Tamil Nadu, India. Agronomy 8, 202. https://doi.org/10.3390/agronomy8100202.

Pan, J., Liu, Y., Zhong, X., Lampayan, R.M., Singleton, G.R., Huang, N., Liang, K., Peng, B., Tian, K., 2017. Grain yield, water productivity and nitrogen use efficiency of rice under different water management and fertilizer-N inputs in South China. Agric. Water Manag. 184, 191–200. https://doi.org/10.1016/j.agwat.2017.01.013.

Qian, H., Zhu, X., Huang, S., Linquist, B., Kuzyakov, Y., Wassmann, R., Minamikawa, K., Martinez-Eixarch, M., Yan, X., Zhou, F., Sander, B.O., Zhang, W., Shang, Z., Zou, J., Zheng, X., Li, G., Liu, Z., Wang, S., Ding, Y., van Groenigen, K.J., Jiang, Y., 2023. Greenhouse gas emissions and mitigation in rice agriculture. Nat. Rev. Earth Environ. 4, 716–732. https://doi.org/10.1038/s43017-023-00482-1.

Rehman, M.Z. ur, Batool, Z., Ayub, M.A., Hussaini, K.M., Murtaza, G., Usman, M., Naeem, A., Khalid, H., Rizwan, M., Ali, S., 2020. Effect of acidified biochar on bioaccumulation of cadmium (Cd) and rice growth in contaminated soil. Environ. Technol. Innov. 19, 101015. https://doi.org/10.1016/j.eti.2020.101015.

Ribas, A., Mattana, S., Llurba, R., Debouk, H., Sebastià, M.T., Domene, X., 2019. Biochar application and summer temperatures reduce N_2O and enhance CH_4 emissions in a Mediterranean agroecosystem: role of biologically-induced anoxic microsites. Sci. Total Environ. 685, 1075–1086. https://doi.org/10.1016/j.scitotenv.2019.06.277.

Sahin, O., Taskin, M.B., Kaya, E.C., Atakol, O., Emir, E., Inal, A., Gunes, A., 2017. Effect of acid modification of biochar on nutrient availability and maize growth in a calcareous soil. Soil Use Manag. 33, 447–456. https://doi.org/10.1111/sum.12360.

Sajjadi, B., Zubatiuk, T., Leszczynska, D., Leszczynski, J., Chen, W., 2019. Chemical activation of biochar for energy and environmental applications - a comprehensive review. Rev. Chem. Eng. https://doi.org/10.1515/revce-2018-0003.

Sharma, A., Singh, Gursharan, Arya, S., 2020. Biofuel from rice straw. J. Clean. Prod. 277, 124101. https://doi.org/10.1016/j.jclepro.2020.124101.

Shaukat, M., Samoy-Pascual, K., Maas, E.D. v L., Ahmad, A., 2019. Simultaneous effects of biochar and nitrogen fertilization on nitrous oxide and methane emissions from paddy rice. J. Environ. Manag. 248, 109242. https://doi.org/10.1016/j.jenvman.2019.07.013.

Shen, Y.L., Yu, S., 2021. The Effects of different agricultural management measures on CH_4 emission from paddy fields in southwest Shandong Province. IOP Conf. Ser.: Earth Environ. Sci. 792, 012051. https://doi.org/10.1088/1755-1315/792/1/012051.

Souza, R., Yin, J., Calabrese, S., 2021. Optimal drainage timing for mitigating methane emissions from rice paddy fields. Geoderma 394, 114986. https://doi.org/10.1016/j.geoderma.2021.114986.

Sriphirom, P., Chidthaisong, A., Yagi, K., Tripetchkul, S., Towprayoon, S., 2020. Evaluation of biochar applications combined with alternate wetting and drying (AWD) water management in rice field as a methane mitigation option for farmers' adoption. Soil Sci. Plant Nutr. 66, 235–246. https://doi.org/10.1080/00380768.2019.1706431.

Sun, H., Zhou, S., Zhang, J., Zhang, X., Wang, C., 2020. Effects of controlled-release fertilizer on rice grain yield, nitrogen use efficiency, and greenhouse gas emissions in a paddy field with straw incorporation. Field Crops Res. 253, 107814. https://doi.org/10.1016/j.fcr.2020.107814.

Wang, B., Gao, F., Li, Y., Lin, C., Cheng, H., Duan, X., 2023. Necessity of introducing particle size distribution of hand-adhered soil on the estimation of oral exposure to metals in soil: comparison with the traditional method. J. Hazard. Mater. 448, 130891. https://doi.org/10.1016/j.jhazmat.2023.130891.

Wang, C., Shen, J., Liu, J., Qin, H., Yuan, Q., Fan, F., Hu, Y., Wang, J., Wei, W., Li, Y., Wu, J., 2019. Microbial mechanisms in the reduction of CH_4 emission from double rice cropping system amended by biochar: a four-year study. Soil Biol. Biochem. 135, 251–263. https://doi.org/10.1016/j.soilbio.2019.05.012.

Wang, H., Zhang, Yan, Zhang, Yaojun, McDaniel, M.D., Sun, L., Su, W., Fan, X., Liu, S., Xiao, X., 2020. Water-saving irrigation is a 'win-win' management strategy in rice paddies – With both reduced greenhouse gas emissions and enhanced water use efficiency. Agric. Water Manag. 228, 105889. https://doi.org/10.1016/j.agwat.2019.105889.

Wang, Y., Xu, L., Liang, S., Li, D., Xia, L., Yu, Y., Wang, J., Tao, Y., Zhang, Y., 2024. Hydrochloric acid-modified biochar enhances nitrogen retention and microbial diversity in mollisols. J. Environ. Chem. Eng. 12, 114129. https://doi.org/10.1016/j.jece.2024.114129.

Wen, P., Tang, J., Wang, Y., Liu, X., Yu, Z., Zhou, S., 2021. Hyperthermophilic composting significantly decreases methane emissions: insights into the microbial mechanism. Sci. Total Environ. 784, 147179. https://doi.org/10.1016/j.scitotenv.2021.147179.

Wu, Q., He, Y., Qi, Z., Jiang, Q., 2022. Drainage in paddy systems maintains rice yield and reduces total greenhouse gas emissions on the global scale. J. Clean. Prod. 370, 133515. https://doi.org/10.1016/j.jclepro.2022.133515.

Wu, Z., Zhang, X., Dong, Y., Li, B., Xiong, Z., 2019. Biochar amendment reduced greenhouse gas intensities in the rice-wheat rotation system: six-year field observation and meta-analysis. Agric. For. Meteorol. 278, 107625. https://doi.org/10.1016/j.agrformet.2019.107625.

Xu, Y., Ge, J., Tian, S., Li, S., Nguy-Robertson, A.L., Zhan, M., Cao, C., 2015. Effects of water-saving irrigation practices and drought resistant rice variety on greenhouse gas emissions from a no-till paddy in the central lowlands of China. Sci. Total Environ. 505, 1043–1052. https://doi.org/10.1016/j.scitotenv.2014.10.073.

Yang, W., Feng, G., Miles, D., Gao, L., Jia, Y., Li, C., Qu, Z., 2020. Impact of biochar on greenhouse gas emissions and soil carbon sequestration in corn grown under drip irrigation with mulching. Sci. Total Environ. 729, 138752. https://doi.org/10.1016/j.scitotenv.2020.138752.

Yu, J., Chang, J.-S., Guo, H., Han, S., Lee, D.-J., 2023. Sodium ions removal by sulfuric acid-modified biochars. Environ. Res. 235, 116592. https://doi.org/10.1016/j.envres.2023.116592.

Zhang, K., Han, X., Fu, Y., Zhou, Y., Khan, Z., Bi, J., Hu, L., Luo, L., 2023. Biochar Coating as a Cost-Effective Delivery Approach to Promoting Seed Quality, Rice Germination, and Seedling Establishment. Plants 12, 3896. https://doi.org/10.3390/plants12223896.

Zhao, Y., Jiang, H., Gao, J., Wan, X., Yan, B., Liu, Y., Cheng, G., Chen, L., Zhang, W., 2024. Effects of biochar application methods on greenhouse gas emission and nitrogen use efficiency in paddy fields. Sci. Total Environ. 915, 169809. https://doi.org/10.1016/j.scitotenv.2023.169809.

Zhou, K., Sui, Y., Xu, X., Zhang, J., Chen, Y., Hou, M., Jiao, X., 2018. The effects of biochar addition on phosphorus transfer and water utilization efficiency in a vegetable field in Northeast China. Agric. Water Manag. 210, 324–329. https://doi.org/10.1016/j.agwat.2018.08.007.